

## Numerical Investigation on Hydrodynamic Characteristics of a Planing Hull

S. L. Chen<sup>a,b</sup>, Q.W. Ma<sup>a</sup> and S. L. Yang<sup>b</sup>

<sup>a</sup> School of Engineering and Mathematical Sciences  
 City University, London, UK

<sup>b</sup> Department of Naval Architecture, Jiangsu University of Science and Technology (JUST)  
 Jiangsu Province, China

### ABSTRACT

The prediction of the total resistance and trim angle of planing crafts at high speed is very important. Since the hydrodynamic characters of high-speed crafts is significantly different from that of displacement-type vessels and need to be further investigated to obtain a better understanding. This issue was widely addressed experimentally so far. Compared with the experiments, the numerical investigation can avoid the tedious and large scale experiments and is able to provide more detailed results of continuous spatio-temporal distribution of physical quantities, such as the wave pattern and the pressure field near the craft. Nevertheless, the related numerical studies on high-speed crafts are relatively limited, mainly due to the complexity involved in this problem, such as wave breaking. This paper presents both experimental and numerical investigations on the hydrodynamic characters of a planing hull craft, including the drag coefficients and trim angle at different forward speeds. The comparison between the numerical and experimental results shows a fairly good agreement. Apart from this, the pressure field and wave pattern around the crafts will be numerically analyzed.

**KEY WORDS:** Hydrodynamic characters; planing craft; Numerical simulation.

### INTRODUCTION

With the development of marine transport, a greater number of high-speed craft are being designed and operated widely. One of them is the planing hull draft. Major concerns in designing the craft are their hydrodynamic properties

There are two ways to understand the hydrodynamics of a planing craft. One way is through the experimental study and another is the through numerical simulation. The experimental studies or model tests for planing craft have been carried out for decades. For examples, Clement and Blount (1963) conducted an extensive model tests on a systematic series (Series 62); Savitsky (2002) developed regression formulas for estimating the hydrodynamic forces acting on planing craft.; and Savitsky et al. (2007) investigated the characteristics of the wetted bottom area and the spray area.

The numerical studies were also carried out by many researchers. Lai and Troesch (1996) and Savander (2002) applied the vortex lattice method (VLM) to study the planing problem and obtained numerical results involving the hydrodynamic pressure, lift and resistance planing craft at various speeds. Zhao et al. (1997) offered a 2.5D (2D+t) analysis of a high-speed planing craft in calm water. Faltinsen (2005) has given details on the hydrodynamics of a planing craft. Doctors (1975) applied finite element method (FPEM) to study the three-dimensional flat planing craft. Cheng and Wellicome (1994) developed a pressure strip method, in which a planing surface is represented by a set of strips of transversely variable pressure placed on the mean free surface. Xie et al. (2005) studied hydrodynamic problem of three-dimensional planing surface by using the vortex theory and the finite element approach. More recently, Wang et al. (2007) used linear pressure distribution over each element with continuous pressure over the length of the planing surface element method (BEM).

The aim of this paper is to discuss the measured resistance and trim angle at different speeds during model tests and then to compare with the numerical simulation results based on commercial CFD software-Fluent. It will be shown that the results are in fairly good agreement with the experimental measurements over a range of Froude numbers.

Table 1. Principal dimensions of planing craft

	Full-scale	Model-scale
Scale ratio	10	1
Length (m)	11.8	1.18
Breadth (m)	3.5	0.35
Draft (m)	0.7	0.07
Initial wetted length $L_S$ (m)	11.2	1.12
Initial wetted area $S_S$ (m <sup>2</sup> )	35.9	0.359
Weight (kg)	7946	7.946
Designed speed (m/s)	13.89	4.39
Froude number	1.3	1.3
Reynolds number	$1.54 \times 10^8$	$4.89 \times 10^6$

## DESCRIPTION OF HULL FORM

The hull form chosen for the present study is 1:10 scaled model of a planing craft of 11.8m long. Its displacement 8.144t and its designed speed is 50 km/h. The craft has a shallow-“V” bottom. The main particulars of the full-scale craft and the scaled model are summarized in Table 1.

## MODEL TESTS

Model tests were carried out in the towing tank at Jiangsu University of Science and Technology with a length of 100m and with a cross section of 6 m (W)× 2 m (D) (the minimum water depth is 0.3m), as shown in Fig. 1. An electrically driven carriage was used to tow ship models, which equipped with force measurement instruments and displacement sensors to provide model’s resistance and trim angle measurement service. Ten towing speeds were chosen from 2.04 m/s to 4.76 m/s to cover the designed speed.



Fig.1 The Towing Tank

To post-process the measured data, several dimensionless parameters are defined as follows. Two of them are the Froude number (Fr<sub>s</sub>) and Reynolds number (Re<sub>s</sub>), which are given, respectively, by,

$$Fr_s = U_c / \sqrt{gL_w} \quad (1)$$

and

$$Re_s = U_c L_w / \nu \quad (2)$$

where,  $U_c$  is the towing speed,  $L_w$  is the wetted length of the ship model corresponding to the towing speed ( $L_w$  is called as corresponding wetted length in this paper and the dimensionless parameters based on it will be called as corresponding Froude number and Reynolds number respectively) and  $\nu$  is the kinematic viscosity coefficient of water. Apart from the above definitions, the Froude number may also be defined in terms of the initial wetted length.  $Fr = U_c / \sqrt{gL_s}$ , where  $L_s$  is the initial wetted length. In addition to the above dimensionless parameters, the resistance ( $R_t$ ) is also expressed in a dimensionless form by:

$$C_d = \frac{R_t}{\frac{1}{2} \rho U_c^2 S} \quad (3)$$

where  $\rho$  is the density of water and  $S$  is the wetted area of the model at

the corresponding speed.

The experimental results (resistance coefficient and trim angle) were presented in Fig.2 and Fig.3. From these figures we can see that when the Froude number less than 1.2 and the Reynolds number less than  $4.2 \times 10^6$  the trim angle increase with the increase of Froude number and Reynolds number. As the trim angle is larger the wet area of the hull becomes smaller. Therefore, the resistance of the craft decreases. This is consistent with what is demonstrated in Fig. 2. It is noted that Chen et al. (2010) have used some of these results to compare with the experimental results of gliding-hydrofoil craft to show the effect of the hydrofoil. They are shown here because the relevant cases will be numerically studied as well.

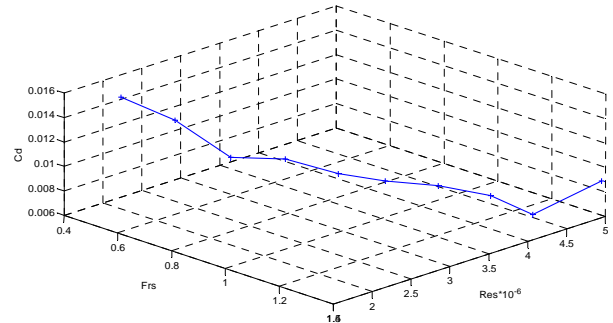


Fig.2 The resistance coefficient at different Froude number

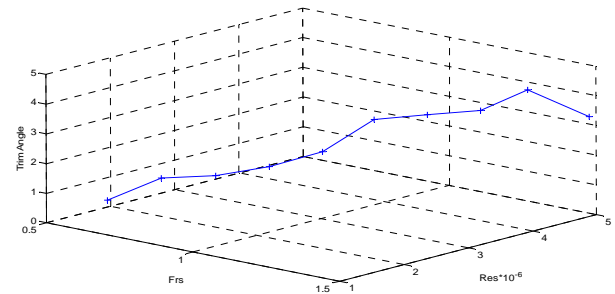


Fig.3 The Trim angle at different Froude number

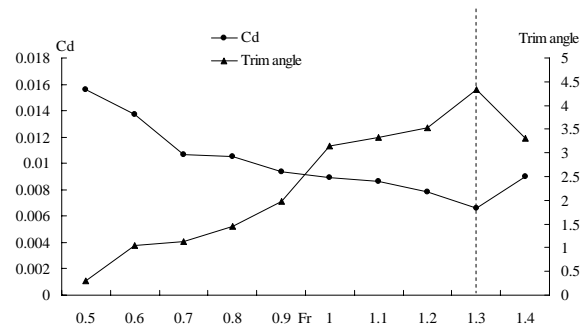


Fig.4 The trim angle at different planing speeds

It is interesting to point out that the resistance reaches its minimum at about  $Fr_s = 1.3$ . Correspondingly, the trim angle at the Froude number

value is 4.3°. For clarity, the two curves are plotted in Fig.4. However, it is noted that the value of optimum trim angle depends on the hull form.

## NUMERICAL MODELS

As indicated above, the commercial software Fluent is employed to perform the numerical analysis of flow around the craft. This is a general-purpose CFD code that has been applied to a broad range of disciplines.

The whole FLUENT software package includes the FLUENT solver with the pre- and post processors. It can use GAMBIT for geometry modelling and mesh generation as well as an additional pre-processor called TGrid for generating volume meshes from existing boundary meshes. The mesh can consist of elements in shapes such as quadrilaterals and triangles for 2-D simulations and hexahedra, tetrahedra, prisms and pyramids for 3-D simulations. Generally, complex unstructured mesh can take a quite long time to be generated. Structured mesh is relatively easy and quick to be generated. It may be adopted for modelling surface ships with high designed speed. Details about what we use are given below.

FLUENT provides four different Volume Of Fluid (VOF) formulations: the geo-reconstruct scheme, the donor-acceptor scheme, the Euler explicit and the implicit scheme. When using it for surface ship modeling, one should test different schemes. In this study, the Euler implicit scheme was chosen.

The ANSYS CFD-Post software is used to post-process its results in several formats including images and flow animations.

### Turbulent model equations

The use of the  $k-\omega$ -based SST turbulence model gives accurate predictions in many cases and it does not consume high computational time in comparison with the higher turbulence models. Furthermore, the preliminary simulations for our cases using other two equations turbulence models showed that the SST turbulence model was the most suitable one for this work.

Thus, the SST turbulent model was used in this study based on the following equations:

$$\frac{\partial(\rho k)}{\partial t} + \frac{\partial}{\partial x_i}(\rho k u_i) = \frac{\partial}{\partial x_j} \left( \Gamma_k \frac{\partial k}{\partial x_j} \right) + G_k - Y_k \quad (4)$$

$$\frac{\partial(\rho \omega)}{\partial t} + \frac{\partial}{\partial x_i}(\rho \omega u_i) = \frac{\partial}{\partial x_j} \left( \Gamma_\omega \frac{\partial \omega}{\partial x_j} \right) + G_\omega - Y_\omega + D_\omega \quad (5)$$

where,  $\Gamma_k$  and  $\Gamma_\omega$  represent the effective diffusivity for  $k$  and  $\omega$ .  $G_k$  represents the generation of turbulence kinetic energy due to mean velocity gradients, and  $G_\omega$  represents the generation of  $\omega$ .  $Y_k$  and  $Y_\omega$  represent the dissipation of  $k$  and  $\omega$  due to turbulence.  $D_\omega$  represents the cross-diffusion term.

### Computation domain, initial and boundary conditions

In simulation, the coordinate system is fixed with the craft and so its speed is replaced by the incoming current of the same speed but in opposite direction. The unsteady problem, if it would have been solved in an earth fixed coordinate system, is then replaced by a steady problem. The no-slip boundary condition is imposed on the ship hull. The free surface is denitrified by a volume fraction which is obtained

by solving the VOF equation. The static pressure condition is applied at the outlet boundary.

Although this is a steady problem in the coordinate system we use, the final location of the free surface at the beginning of the solution is unknown. Therefore, we still solve the problem as an unsteady one, though the results at the intermediate steps may not be used. For this purpose, it needs an initial location of the free surface to start the calculations. The initial location of the free surface is specified by defining the volume fraction function.

To save the computational time, only half of the domain was considered and the solutions for the other half are deduced by implementing the symmetric condition.

### Computational method

To solve the governing fluid equations, the fluid domain is subdivided into a finite number of cells and then governing equations are changed into a set of algebraic equations. A high-resolution numerical scheme (Barth and Jespersen, 1989) is used for discretizing the advection terms to reduce numerical diffusion. A linear interpolation scheme is used for interpolating the pressure, while the velocity was interpolated using a tri-linear numerical scheme. The root mean-square (RMS) criterion with a residual target value of 0.0001 was employed for checking the convergence of the solutions.

During the calculation the resistant force is checked. Convergence is achieved, if the changes of the wave-making resistance are less than a specified value.

## RESULTS AND COMPARISONS

A Cartesian coordinate system  $o$ - $xyz$  fixed to the body is established, with its  $y$ -axis in the opposite direction of gravity,  $y=0.05m$  at the undisturbed free surface and  $x$ -axis in the longitudinal direction towards the stern of the ship (Fig.5).



Fig.5 Planing craft and coordinate system

The computational domain extends 4.5 ship length downstream, 1.5 ship lengths upstream, 1.5 ship length in the  $z$ -direction, 1 ship length in the positive  $y$ -direction and 2 ship length in the negative  $y$ -direction. Fig.6 and Fig.7 show the grid of the computational domain and the planing hull surface.

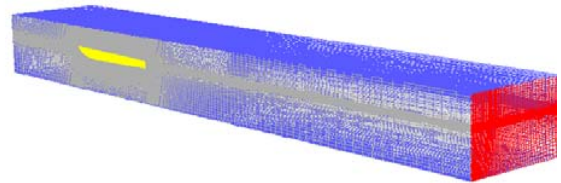


Fig.6 Computational grid with 705490 elements

The computational domain was discretized using hexahedral (brick) elements and tetrahedral elements. The hexahedral meshes are much

more computationally efficient than tetrahedral meshes. Typically, a hexahedral mesh requires half the resolution in each of the three directions. Tetrahedral elements must be used in portions of the geometry that are too complex to use hexahedral elements. The solution is then calculated on the hybrid tetrahedral-hexahedral mesh. This allows solution of problems in arbitrarily complex geometries while realizing the high efficiency of hexahedral elements.

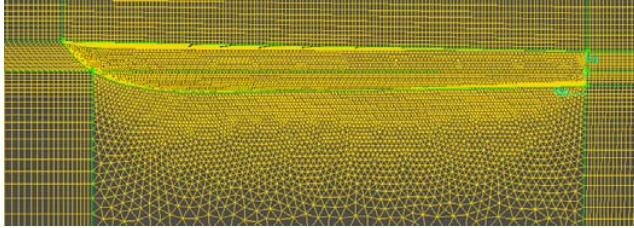


Fig.7 Computational grid near planing craft

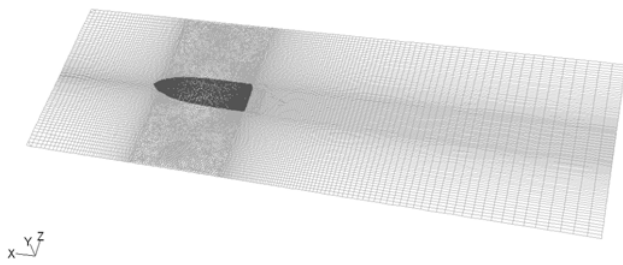
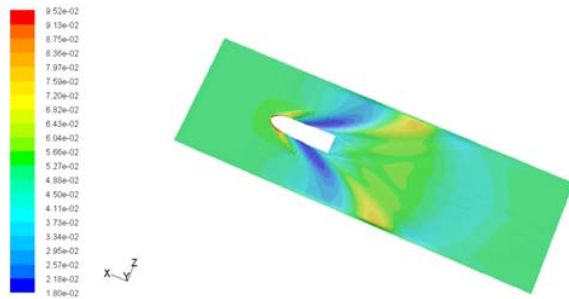


Fig.8 Computational panels on the water-surface around the planing craft hull

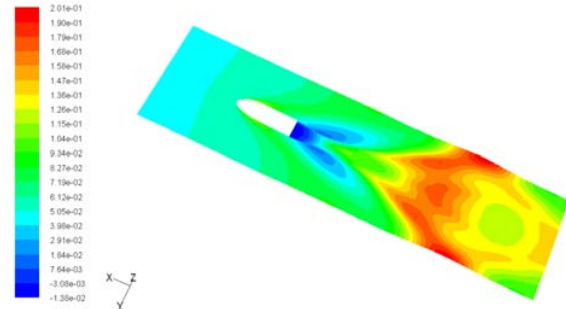
The numerical results are obtained on a single computer Pentium IV 2.4 GHz and 2Gb RAM. The solver has typically taken about 10 hours for reaching the converged solution.

### Wave pattern

The wave profile around the planing craft is given in Fig.9 and Fig. 10 for the Froude numbers of 0.5 and 1.0, respectively. These are top views of the free surface profiles. It is noted that the free surface wave is well developed and does not change significantly if longer calculation is performed.



(a) Fr=0.5



(b) Fr=1.0

Fig.9 Wave patterns generated by a planing craft advancing at different Fr

It can be seen that the wave patterns are very different at the lower and higher Froude numbers. At the lower Froude number, the wave spreads in a relative larger area and maximum wave height occurs at the bow area. On the other hand, at the relative higher Froude number, the wave spread in a narrower area and the maximum wave height occurs behind the ship.

### Resistance

The experimental results and the corresponding computed values of resistance coefficient are compared in Fig.10 for 8 values of Froude number from 0.6 to 1.3. As can be seen from Fig.10, the numerical values of  $C_d$  have the same trend to that of experimental data as Froude number increases. The agreement between them for a wide range of Froude number is satisfactory.

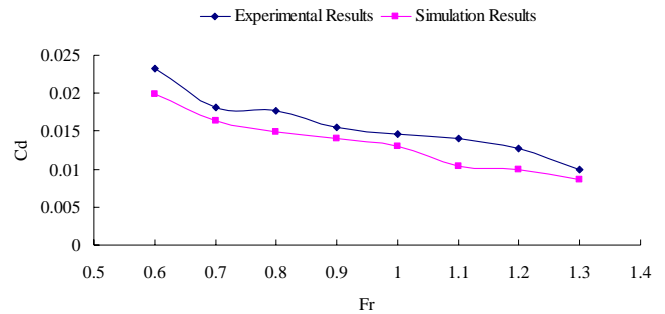


Fig.10. Comparison of the resistance coefficients ( $C_d$ )

### CONCLUSIONS

The incompressible free surface flow around the planing craft has been investigated using the numerical modeling and physical tests. The numerical results have been compared with the experimental results and shown to be in reasonable agreement. It has been observed that the trim angle is about  $4.3^\circ$  where the resistant (drag) force is minimum in the cases studied at about the Froude number being at 1.3.

### REFERENCES

Chen, S.L, Yang, S.L. and Ma, Q.W. (2010). "An experimental study on hydrodynamic characteristics of gliding-hydrofoil craft." Journal of Marine Science and Technology.  
 Cheng, X., Wellicome, J.F. (1994). "Study of planing hydrodynamics using strips of transversely variable pressure." Journal of Ship

- Research Vol 38, No2, pp30–41.
- Clement, E.P. and Blount, D.L. (1963), “Resistance tests of systematic series of planing hull forms.” SNAME Transactions 71, pp. 491-579.
- Doctors, L.J. (1975). “Representation of three dimensional planing surfaces by finite elements.” Proceedings of the First Conference on Numerical Ship Hydrodynamics, pp. 517–537.
- Faltinsen, O.M. (2005), “Hydrodynamics of High-Speed Marine Vehicles.” Cambridge University Press, New York.
- Lai, C., Troesch, A.W. (1996). “A vortex lattice method for high speed planing.” International Journal of Numerical Method in Fluids Vol 22, pp495–513.
- Savander, B.R., Scorpio, S.M., Taylor, R.K. (2002). “Steady hydrodynamic of planing surface.” Journal of Ship Research Vol 46, No 4, pp248–279.
- Savitsky, D. (1992). “Overview of planing hull developments.” In Proc.HPMV’92, pp. PC1–PC14.
- Savitsky, D., DeLorme, M.F. and Raju, D. (2007). “Inclusion of whisker spray drag in performance prediction method for high-speed planing hulls,” Journal of Marine Technology Vol.44, pp.35-56.
- Wang, X., Day, H., Alexander, A. (2007). “Numerical instability in linearized planing problems.” International Journal of Numerical Methods Engineering Vol 70, pp840–875.
- Xie, N., Vassalos, D., Jasionowski, A. (2005). “A study of hydrodynamics of three-dimensional planing surface.” Journal of Ocean Engineering Vol 32, pp1539–1555.
- Zhao, R., Faltinsen, O.M., Haslum, H.A. (1997). “A simplified nonlinear analysis of a high-speed planing craft in calm water.” In: Proceedings of the Fourth International Conference on Fast Sea Transportation, Australia.